Development and optimization of a pantograph-based robotic gripper for industrial applications*

Vitaliy Korendiy[1,†], Oleksandr Kachur[1,†], Andy Augousti[2,†], Olena Lanets[2,*,†], Mykhailo Pylyp[1,†] and Roman Karpyn[1,†]

[1] *Lviv Polytechnic National University, 12, Stepan Bandera str., 79013, Lviv, Ukraine*

[2] *Kingston University, Department of Mechanical Engineering, Faculty of Engineering, Computing and the Environment, Roehampton Vale, London SW15 3DW, United Kingdom*

Abstract

This paper presents the kinematic and force analysis of a pantograph-based industrial gripper designed for transportation cylindrical parts in automated systems. The gripping mechanism was modeled and validated using numerical simulations in Mathematica and SolidWorks Motion. The results show that the gripper provides stable and accurate operation within the design operating range, applying a maximum gripping force of 45 N. Compared to conventional gripping mechanisms, the proposed design provides improved force distribution and efficient energy utilization. The study confirms the effectiveness of the pantograph-based gripper for industrial automation applications that require stable and controllable gripping forces.

Keywords

industrial gripper, pantograph mechanism, kinematic analysis, force analysis, automation

1. Introduction

Automated lines in factories significantly increase production efficiency, ensuring accuracy, speed and minimizing human intervention in technological processes. Thanks to the integration of robotic manipulators, conveyor systems and software control, modern production lines are able to adapt to changes in production requirements, reducing costs and improving the quality of the final product [1].

Industrial robots equipped with grippers are widely used in manufacturing, logistics, and assembly lines to handle components, optimize production processes, and reduce human intervention [2]. The study [3] emphasizes the need to develop hybrid solutions and integrate predictive modeling to improve the efficiency of modern robotic grippers.

Robotic grippers can be classified into several categories based on their actuation mechanisms and operating principles. Namely, they are mechanical grippers, pneumatic grippers, and electromechanical grippers. They are key elements of modern industrial manipulators and are widely used in manufacturing processes for automated gripping, moving and stacking of objects [4].

Although existing gripping technologies have been successfully integrated into various industrial applications, they have certain limitations and development prospects [5, 6].

SMARTINDUSTRY-2025: International Conference on Smart Automation & Robotics for Future Industry, April 3 - 4, 2025, Lviv, Ukraine

1* Corresponding author.
† These authors contributed equally.These authors contributed equally.
vitalii.m.korendii@lpnu.ua (V. Korendiy); oleksandr.y.kachur@lpnu.ua (O. Kachur); augousti@kingston.ac.uk (A. Augousti) ; o.lanets@kingston.ac.uk (O. Lanets); mykhailo.v.pylyp@lpnu.ua (M. Pylyp); roman.b.karpyn@lpnu.ua (R. Karpyn)
0000-0002-6025-3013 (V. Korendiy); 0000-0003-2263-6360 (O. Kachur); 0000-0003-3000-9332 (A. Augousti); 0000-0001-7149-0957 (O. Lanets); 0009-0003-7964-0624 (M. Pylyp); 0009-0005-1695-492X (R. Karpyn)

The choice of gripper design largely depends on the specifics of the tasks performed, the shape of the object, the requirements for accuracy and stability of the gripper, as well as on energy efficiency and production costs [7].

Modern developments of grippers are aimed at optimizing the kinematics of the mechanism, improving controllability and increasing adaptability to different types of objects, which allows for effective performance of "pick and place" tasks in production processes [8].

For example, pneumatic grippers demonstrate high speed but require additional compressor systems and have limited grip force and position control capabilities [9]. Existing developments combine different approaches, such as the combination of soft and hard elements in grippers, which demonstrates high efficiency in manipulating objects of different shapes and sizes [10].

Research [11] demonstrates that kinematic analysis plays a key role in the design of robotic grippers, allowing for accurate prediction of motion transmission and force characteristics. This analysis can be used to optimize the design to provide adaptive gripping of objects of different shapes and stiffness without the use of additional force sensors.

Research work [12] also highlights design solutions of a new linear serial elastic gripper (LSEA-RG), which can adaptively grip objects of different shapes and sizes by controlling the gripping force. The experiments confirmed that LSEA-RG can estimate the gripping force without sensors on the fingertips and adaptively grip objects of different stiffness.

Despite significant progress in the development of robotic grippers, research in this field reveals a number of problem areas that need to be further addressed. Precise control of gripping force remains a challenge due to nonlinear effects such as friction and airflow dynamics in pneumatic grippers. Furthermore, while finger position control has reached an acceptable level in electric grippers, pneumatic mechanisms still suffer from poor controllability in both force and positioning, which limits their effectiveness [13].

The development of robotic grippers requires the introduction of new design concepts, including flexible mechanisms, topology optimization, material selection, and drive methods, to ensure grip reliability and adaptability.

The main objective of this research is to develop a high-precision, energy-efficient and adaptive robotic gripper. The proposed design includes a pantograph-based mechanism combined with a lead screw drive, which provides precise force control and flexible adaptation to objects of different sizes. By integrating this design, we aim to overcome the limitations of traditional grippers and provide an effective solution for industrial automation applications.

2. Materials and Methods

The design and performance of robotic grippers is based on an effective combination of kinematic structure, force distribution, and energy efficiency. This section outlines the methodological framework used to design and analyze the proposed gripping mechanism. The study includes kinematic modeling, force analysis, and numerical verification to evaluate the adaptability and effectiveness of the gripper. Computational simulations were performed in Mathematica and SolidWorks Motion to verify the theoretical conclusions.

2.1. Description of the gripper design and its functional components

For this research, a stationary robot (Figure 1) was designed to perform reloading operations based on a SCARA-type manipulator and a pantograph gripper. The robot in Figure 1 is mounted on a vertical column 1, which is attached to the foundation. A mounting plate 2, with several holes for bolted connections, is used to install the robot on the column. Four clamps 3 are also installed on plate 2 to fix the vertical guides 4 of the vertical lifting mechanism of the manipulator. The drive of this mechanism is carried out from a stepper motor 5, through a toothed belt transmission 6 to a screw shaft 7. For the upper fixation of guides 4 and shaft 7, plate 8 with a set of clamps 3 is used. The screw 7 is installed in the bearing supports and drives the nut 9 attached to the vertical lifting plate of the manipulator. Guide (linear) bearings 10 are also fixed on it, which provide vertical movement of the plate along four guides. To drive the first link 11 of the manipulator into rotational motion, stepper motor 12 and a gear-belt transmission 13 are used. Another electric motor 14 through a gear-belt transmission 15 ensures the rotation of the second link 16 of the manipulator relative to the first link 11 around the bearing units 17. At the free end of the link 16, mechanisms for rotation and vertical movement of the gripper are installed. The rotation of the gripper in the horizontal plane is carried out using a stepper motor 18 and a gear 19. The mechanism for vertical movement of the gripper 20 is driven by an electric motor 21 through a gear-belt transmission 22. At the same time, the gripper 20 can move along vertical guides 23.

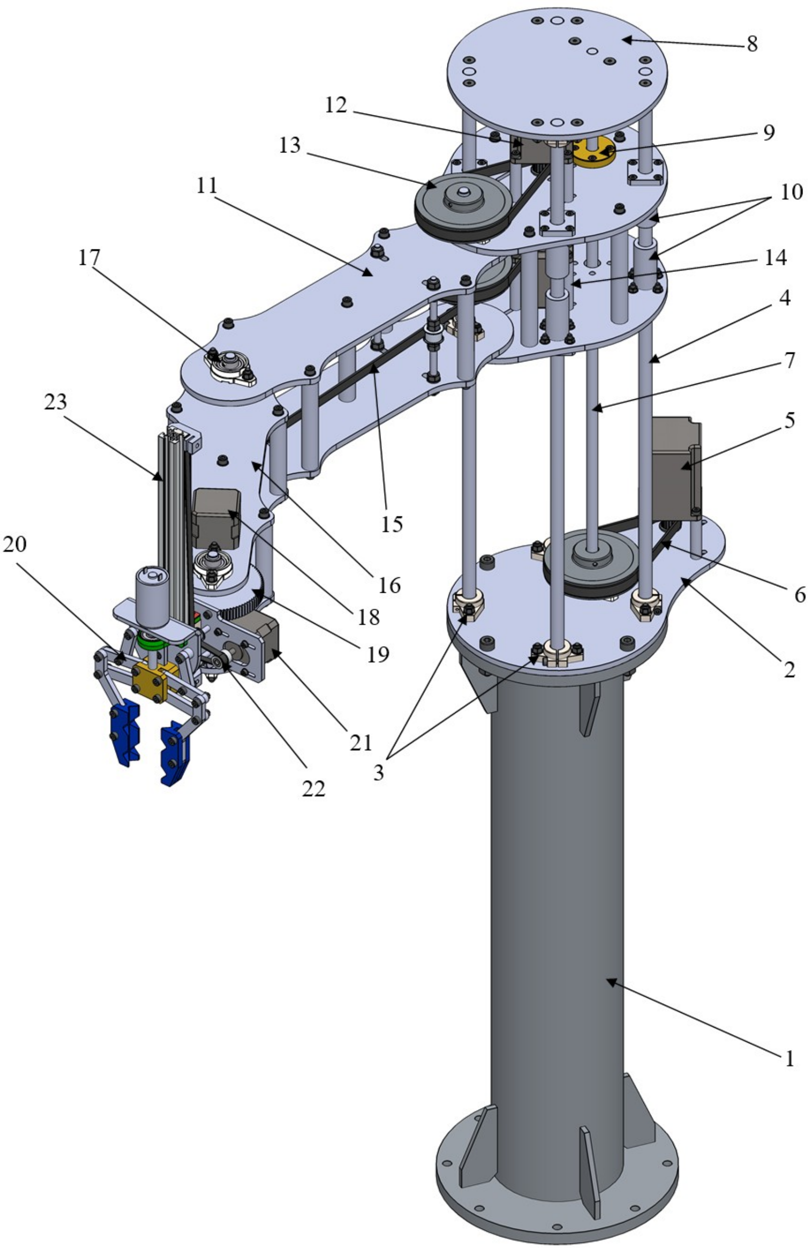

Figure 1: Overall design of the developed industrial robot

The main object of design in this study is the gripper, the general view of which is shown in Figure 2. Through the mounting plate 1, it is connected to the rotary gear sector, which provides the possibility of rotation around the bearing assembly, which is installed on the free end of the second section of the SCARA-type manipulator. A stepper motor 2 is fixed on plate 1, which, through a system of one drive and two tension pulleys 3, drives the belt 4, which, in turn, ensures the vertical movement of the gripper plate 5 along the profile guide 6. The gripper itself is a lever pantograph (parallelogram) mechanism, the links of which are driven by the servomotor 7 through a screw-nut transmission 8. The gripper is designed to move cylindrical parts with a diameter of 10 to 40 mm and a length of 20 to 150 mm.

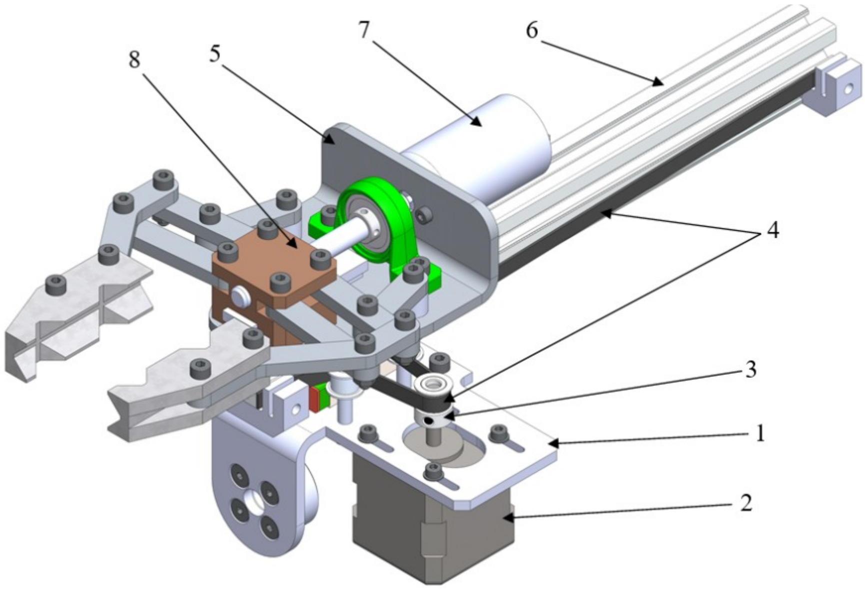

Figure 2: General view of the designed gripper

2.2. Structural Analysis of the Gripper Mechanism

The developed model of the gripper movement is based on the transmission of torque from the electric motor through the screw shaft to the nut *A*, which plays a key role in the functioning of the mechanism (Figure 3). Nut *A* is pivotally connected to four levers (DB, D_1B_1, GE, G_1E_1), which form a pantograph kinematic chain. This design ensures the vertical position of the gripper jaws, regardless of their degree of opening or closing.

Table 1
Types of kinematic joints in a mechanical system

#	Designation	Links forming a pair	Type	Class
1	O	Fixed Frame – OC	Revolute	5
2	O_2	Fixed Frame – O_2C_1	Revolute	5
3	C	$OC - DB$	Revolute	5
4	C_1	$O_2C_1 - D_1B_1$	Revolute	5
5	D	$DB - A$	Revolute	5
6	D_1	$D_1B_1 - A$	Revolute	5
7	B	$DB - BEHK$	Revolute	5

8	B_1	$D_1B_1 - B_1E_1H_1K_1$	Revolute	5
9	G	$GE - A$	Revolute	5
10	G_1	$G_1E_1 - A$	Revolute	5
11	E	$GE - BEHK$	Revolute	5
12	E_1	$G_1E_1 - B_1E_1H_1K_1$	Revolute	5
13	A	Fixed Frame – A	Prismatic	5

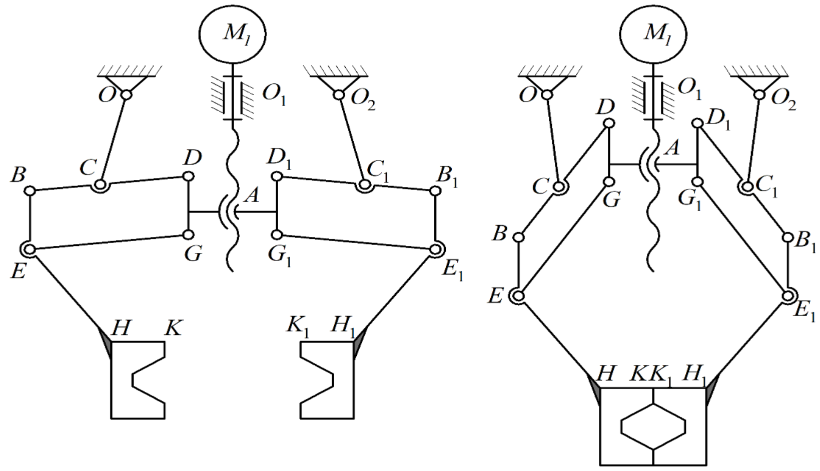

Figure 3: Calculation diagram of a pantograph gripper

The *OC*, O_2C_1 mechanisms performs the function of controlling the convergence and divergence of the jaws, allowing their synchronous movement in accordance with the movement of the nut.

During the movement of the nut *A* up along the screw shaft, the jaws converge, while the reverse movement of the nut down ensures the divergence of the jaws.

To determine the degree of freedom (DOF) of the mechanism, the Chebyshev formula for flat kinematic chains was used

$$W = 3n - 2p_5 - p_4, \tag{1}$$

where *n* is the number of moving links of the mechanism, p_5 is the number of single-moving kinematic pairs, p_4 is the number of double-moving kinematic pairs.

Based on the structural model in Figure 3, it is established that the mechanism has 9 moving links and 13 single-moving kinematic pairs (Table 1). There are no higher kinematic pairs in the gripping mechanism, so $p_4 = 0$. Thus, the DOF is W = 1. This means that the mechanism is characterized by one DOF.

To define class of the mechanism, we decompose the mechanism into mechanisms of the 1st class and structural groups in the reverse order of its assembly (see Figure 4).

To verify the class of structural groups of the gripper mechanism, its DOF was determined, taking into account 4 moving links (*DG (A), DB, GE, BE*) and 6 single-moving kinematic pairs (*C, D, B, G, E, A*) (see Figure 4) (W = 0).Thus, we can conclude that the gripper mechanism is indeed a class IV mechanism. Its structural formula is written as follows

$$I(O,C) \leftarrow IV(BDGE); \tag{2}$$

$$I(O_2,C_1) \leftarrow IV(B_1D_1G_1E_1). \tag{3}$$

Based on the structural analysis, it can be concluded that to uniquely determine the position of the gripper jaws (points K and K_1) at any given moment, it is sufficient to know the law of variation of a single generalized coordinate, specifically, the position of the lead screw nut.

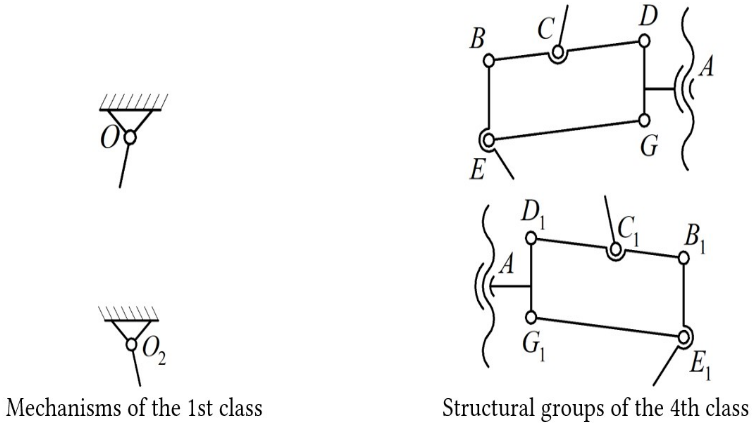

Figure 4: Structural groups of the gripper mechanism.

2.3. Kinematic analysis of the gripper mechanism

To analyze the kinematics of the gripper mechanism, we choose an inertial (stationary) reference frame, which is presented in the form of a flat Cartesian coordinate system with the center in the hinge O_1, which is located on the axis of the screw of the gripper drive mechanism (Figure 5). The vertical axis O_y coincides with the axis of the drive screw. As a generalized coordinate, we will take the vertical position of the nut A is y_A relative to the hinge O_1. The initial data are the geometric parameters of all links and the coordinates of the hinges O and O_2.

A kinematic analysis is conducted to establish the maximum and minimum distance between the gripper jaws depending on the movement of the drive mechanism nut. According to the adopted data of the study, the gripper should provide movement of cylindrical parts with a diameter of 10 to 40 mm.

Let's write the expressions for finding the coordinates of the hinges D and G

$$x_D=-l_{AL},\ y_D=y_A+l_{LD};$$
$$x_G=-l_{AL},\ y_G=y_A-l_{LG}. \tag{4}$$

To find the coordinates of hinge C, we derive the following geometric relations (see Figure 5)

$$l_{OD}=\sqrt{}\left(\left(x_D-x_O\right)^2+\left(y_O-y_D\right)^2\right);$$
$$\alpha=\operatorname{arctg}\left(\left(x_D-x_O\right)/\left(y_O-y_D\right)\right);$$
$$\gamma=\arccos\left(\left(\left(l_{OC}\right)^2+\left(l_{OD}\right)^2-\left(l_{CD}\right)^2\right)/\left(2\cdot l_{OC}\cdot l_{OD}\right)\right); \tag{5}$$
$$\beta=\gamma-\alpha;$$
$$x_C=x_O-l_{OC}\cdot\sin\beta,\ y_C=y_O-l_{OC}\cdot\cos\beta.$$

Let's find the coordinates of points B, E, H, and K:

$$x_B=x_D-\left(x_D-x_C\right)\cdot l_{DB}/l_{CD},\ y_B=y_D-\left(y_D-y_C\right)\cdot l_{DB}/l_{CD};$$
$$x_E=x_B,\ y_E=y_B-l_{BE}; \tag{6}$$
$$\varphi=\pi-\theta;$$

$$x_H = x_E + l_{EH} \cdot \sin\varphi,\ y_H = y_E - l_{EH} \cdot \cos\varphi;$$

$$x_K = x_H + l_{KH},\ y_K = y_H.$$

The last stage of the kinematic analysis is to determine the distance between the gripping jaws. Considering that the gripper consists of two symmetrically arranged pantograph mechanisms (Figure 4), we can state that the total distance between the jaws will be

$$\Delta x_K = 2 \cdot \vee x_K \vee. \tag{7}$$

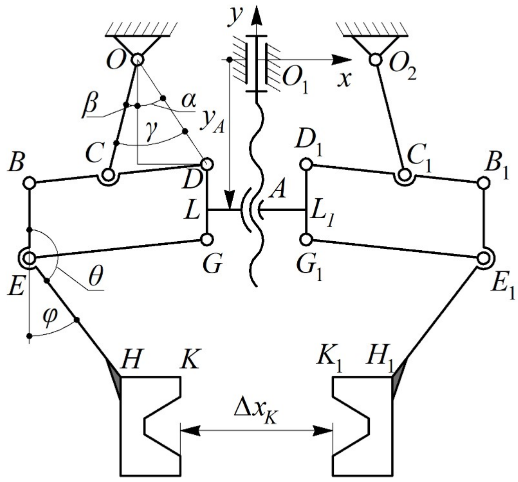

Figure 5: Calculation diagram of the gripper mechanism for analyzing its kinematics.

Using the derived equations of motion of the gripper jaws, it is possible to built the trajectories of their motion, as well as calculate the velocities and accelerations at any point of the trajectory with a known law of change of the generalized coordinate.

3. Modeling and results

To confirm the theoretical assumptions and assess the performance of the developed gripping mechanism, computational and numerical modeling was carried out.

3.1. Modeling gripper kinematics in Mathematica and SolidWorks software

Based on the developed solid-state model of the gripper (see Figure 2), designed in the SolidWorks software product, and analytical dependencies derived above, a simulation of the movement of the gripper jaws was performed in the Mathematica software product. For the simulation, the corresponding geometric parameters presented in Table 2 of the gripper links were set.

Table 2
Parameters of the Gripper Links

Designation	Parameters	Units
l_{AL}	12.5	mm
l_{LD}	11.5	mm
l_{LG}	7.5	mm

x_O	-30	mm
y_O	0	mm
l_{OC}	30	mm
l_{CD}	25	mm
l_{DB}	45	mm
l_{BE}	19	mm
l_{EH}	37.8	mm
l_{KH}	15	mm
θ	142.5	°

Based on the results of substituting the specified geometric parameters into the analytical expressions derived above, the trajectories of the gripper jaws were obtained (Figure 6) and a graph of the dependence of the distance between the jaws on the position of the nut of the drive screw mechanism are shown in Figure 7.

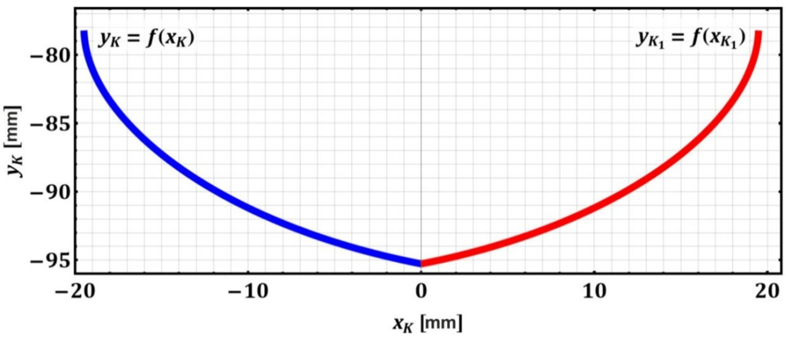

Figure 6: Trajectories of the gripper jaws, modeled in the Mathematica software product according to the derived analytical dependencies.

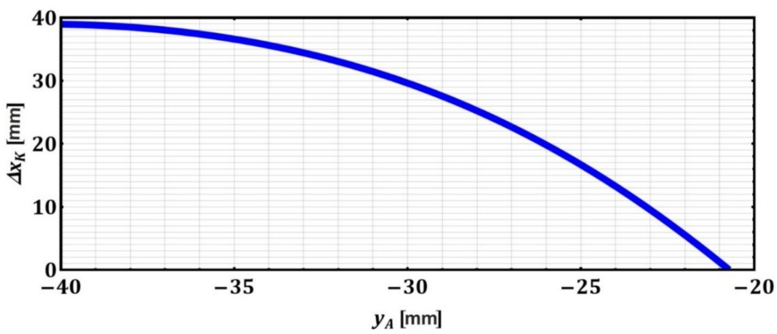

Figure 7: Graphical dependence of the distance between the gripper jaws on the position of the nut of the drive screw mechanism.

The results of the numerical simulation show that the maximum distance between the gripping jaws reaches approximately 39 mm when the lead screw nut is located at 40 mm from the mounting plate. According to the solid-state simulation data carried out in the SolidWorks software, the distance of 39 mm between the jaws will allow gripping parts with a circular crosssection with a diameter of up to 40.8 mm when the gripper approaches from the end of the part (see Figure 8). The minimum distance between the jaws is zero when they are fully closed, with a distance from the nut to the mounting plate of about 21 mm. Considering the design of the gripper jaws, the results of solid-state simulation showed that when the jaws are fully closed, the minimum diameter of the part to be gripped is about 9.5 mm (see Figure 8). Thus, the results obtained confirm that the gripping mechanism provides the ability to work with cylindrical objects in a given range.

To verify the correctness of the derived analytical dependencies and the results of numerical modeling in the Mathematica software, virtual experiments of the movement of the gripper mechanism were conducted in the Motion application of the SolidWorks program, which is shown in Figure 9. As a result of moving the nut of the drive screw mechanism by a distance of 19 mm, each of the gripper jaws moved from their contact state by approximately 19.2 mm in the horizontal direction and by 15.1 mm in the vertical direction. The virtual trajectory of the jaws movement fully corresponds to the theoretically derived trajectory. The maximum distance between the jaws in the open state of the gripper is about 38.4 mm, which practically coincides with the data of mathematical modeling.

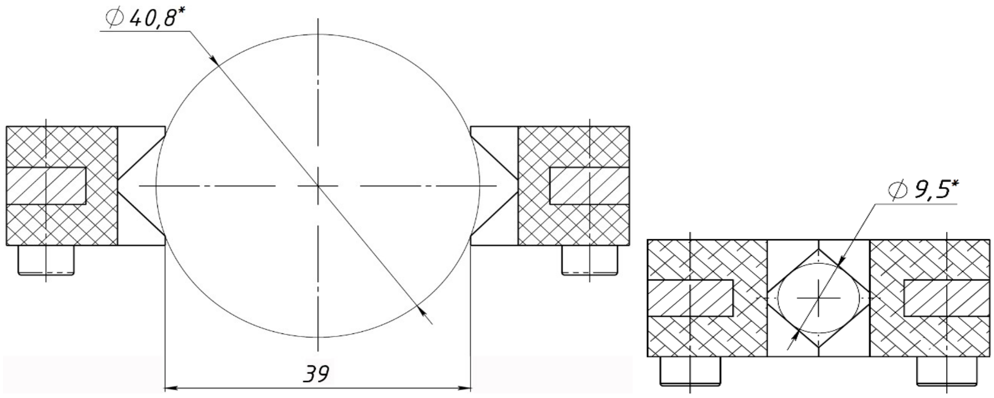

Figure 8: Results of checking the geometric parameters of the gripper jaws in the SolidWorks software product.

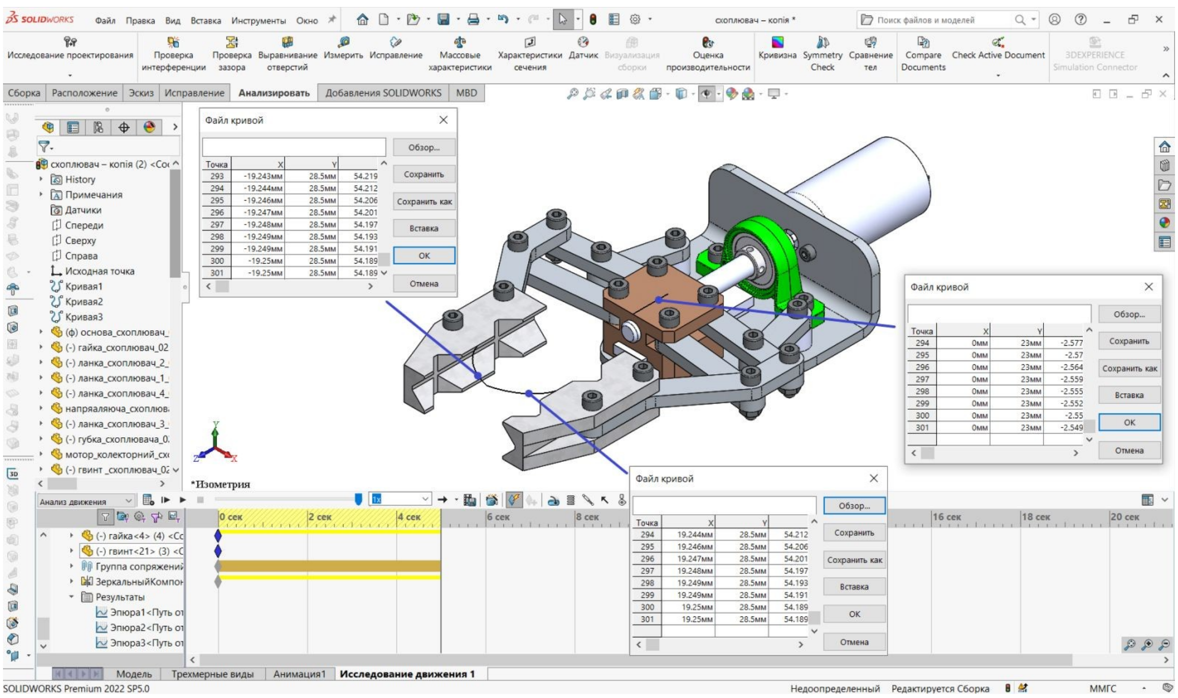

Figure 9: Results of a virtual experiment conducted in SolidWorks Motion.

3.2. Force analysis of the gripper mechanism

To conduct the force analysis, the required gripping force necessary, for the secure transportation of the object within the gripper jaws, is determined. This estimation is based on the assumed mass and weight (Eq. 8) of a cylindrical workpiece with maximum dimensions (d_{max}=40 mm, l_{max}=150 mm), manufactured from structural steel St3 (GOST 380-2005), which has similar characteristics to S235JR (EN 10025-2). The analysis aims to ensure reliable fixation and stability of the object during handling and transportation.

$$m_{max}=(\pi(d_{max})^2)/4\cdot l_{max}\cdot\rho=3.14/4\cdot 0.15\cdot 7850\approx 1.5\,kg;\quad G_{max}=m_{max}\cdot g=1.5\cdot 9.81\approx 15\,N, \tag{8}$$

where ρ =7850 kg/m^2 is steel density, g = 9.81 m/s^2 is the acceleration due to gravity.

Knowing the material of the gripper sponges is polyurethane rubber, we can determine the approximate coefficient of friction between the surfaces of the sponge and the part. The coefficient of friction between polyurethane rubber and steel St. 3 can vary depending on specific conditions, such as surface cleanliness, the presence of lubricant, temperature and other factors. In general, for dry conditions the coefficient of friction between polyurethane rubber and steel is approximately f = 0.5...0.7. [14].

Taking the coefficient K_n of possible overloads up to 150% in the process of accelerated lifting of parts, we will determine the necessary pressing force of the gripper jaws from the condition of ensuring the necessary friction force

$$N_{pr}=(K_n\cdot G_{max})/f=(1.5\cdot 15)/0.5=45\,N. \tag{9}$$

To ensure the possibility of designing individual reactions in the links of the gripper mechanism, we will additionally determine the angles λ, χ and ψ using Eq. 10. (see Figure 10)

$$\begin{gathered}\lambda=arctg((y_O-y_D)/(x_D-x_O));\\ \chi=\arccos(((l_{CD})^2+(l_{OD})^2-(l_{OC})^2)/(2l_{CD}l_{OD}));\\ \psi=\chi-\psi.\end{gathered} \tag{10}$$

Let us write the equation of equilibrium for the lever *BEHK* (see Figure 10)

$$\begin{gathered}\sum F_{kx}=0:-N_{pr}+R_{EG}\cdot cos\psi-X_B=0;\\ \sum F_{ky}=0:-0.75G_{max}+R_{EG}\cdot sin\psi+Y_B=0;\\ \sum M_B(F_k)=0:\\ -N_{pr}\cdot(l_{(BE)}+l_{EH}\cdot cos\varphi+l_{KM})+R_{EG}\cdot cos\psi\cdot l_{BE}-0.75\cdot G_{max}\cdot(l_{EH}\cdot sin\varphi+l_{KH})=0.\end{gathered} \tag{11}$$

Solving this system of equations (Eq. 11), we can determine the unknown reactions in the hinge *B* and in the rod *EG*

$$\begin{gathered}R_{EG}=(N_{pr}((l_{(BE)}+l_{EH}\cdot cos\varphi+l_{KM})+0.75G_{max}\cdot(l_{EH}\cdot sin\varphi+l_{KH})))/(cos\psi\cdot l_{BE});\\ X_B=-N_{pr}+R_{EG}\cdot cos\psi;\\ Y_B=0.75\cdot G_{max}-R_{EG}\cdot sin\psi.\end{gathered} \tag{12}$$

Let us write the equilibrium equation for the lever *BCD* (see Figure 10)

$$\begin{gathered}\sum F_{kx}=0:X_D+R_{CO}\cdot\sin\beta+X'_B=0;\\ \sum F_{ky}=0:Y_D+R_{CO}\cdot\cos\beta-Y'_B=0;\\ \sum M_D(\vec{F}_k)=0:X'_B\cdot l_{DB}\cdot\cos\psi-R_{CO}\cdot\sin(\pi-\gamma-\chi)l_{CD}+Y'_B\cdot l_{DB}\cdot\sin\psi=0.\end{gathered} \tag{13}$$

Solving this system of equations (Eq. 13), we can determine the unknown reactions in the hinge D and in the rod OC:

$$R_{CO}=(X'_B \cdot l_{DB} \cdot \cos\psi+Y'_B \cdot l_{DB} \cdot \sin\psi)/(\sin(\pi-\gamma-\chi) \cdot l_{CD});$$
$$X_D=-R_{CO} \cdot \sin\beta-X'_B; \tag{14}$$
$$Y_D=-R_{CO} \cdot \cos\beta+Y'_B.$$

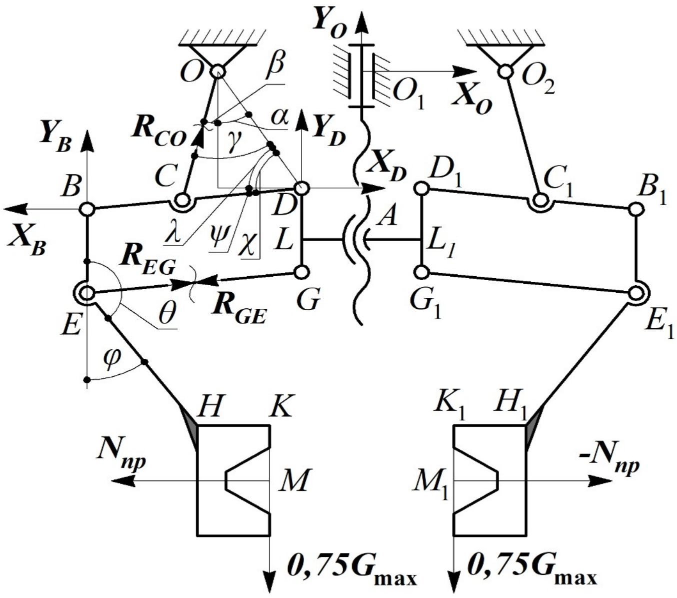

Figure 10: Calculation diagram of the gripper mechanism for its force analysis.

Considering that the horizontal components of the reactions from both parts of the pantograph mechanism will be balanced, we can state that the horizontal reaction in the hinge O_1 will be equal to zero. To find the vertical reaction Y_{O1} in the hinge O_1, we write the following equilibrium equation for the screw O_1A (see Figure 10)

$$\sum F_{ky}=0:-Y'_D-R_G \cdot \sin\psi+Y_{(O_1)}=0;$$
$$Y_{(O_1)}=Y'_D+R_G \cdot \sin\psi. \tag{15}$$

In the above formulas, the reactions X_B, Y_B, Y_D, R_{GE} are equal in magnitude to the corresponding reactions X_B, Y_B, Y_D, R_{EG} but opposite in direction.

Substituting the calculated values of the active forces GH_{max} and N_{pr}=45N into the analytical expressions derived above, we can build graphical dependences of the reactions in the hinges and rods of the pantograph mechanism of the gripper on the position y_A of the nut of the drive screw mechanism. For this, we will use the geometric parameters of the mechanism adopted in our research and the Mathematica software, and additionally the following size l_{KM}=12.5mm will be specified.

The simulation results are shown in Figure 11. As can be seen, the horizontal reaction in the hinge B practically does not change when the adjusting nut is moving, and it is about 120 N. The vertical reaction in the hinge B reaches a maximum value of about 230 N. The reaction in the rod O_1C during the jaws tightening process decreases from 300 N to −230 N. The rod EG is constantly under the action of a tensile force, which varies in the range from 165 N to 290 N. The horizontal reaction in the hinge D during the jaws movement is in the range of 120...200 N, while the vertical reaction reaches 280 N when the jaws are spread apart and goes to zero when they are brought together. The vertical force on the screw of the drive screw mechanism during the jaws tightening process changes from −280 N to 240 N, causing both the screw to stretch and compress (depending on the jaws position). The obtained dependencies were used in the process of designing the corresponding hinges and levers of the gripper in order to ensure its strength during operation.

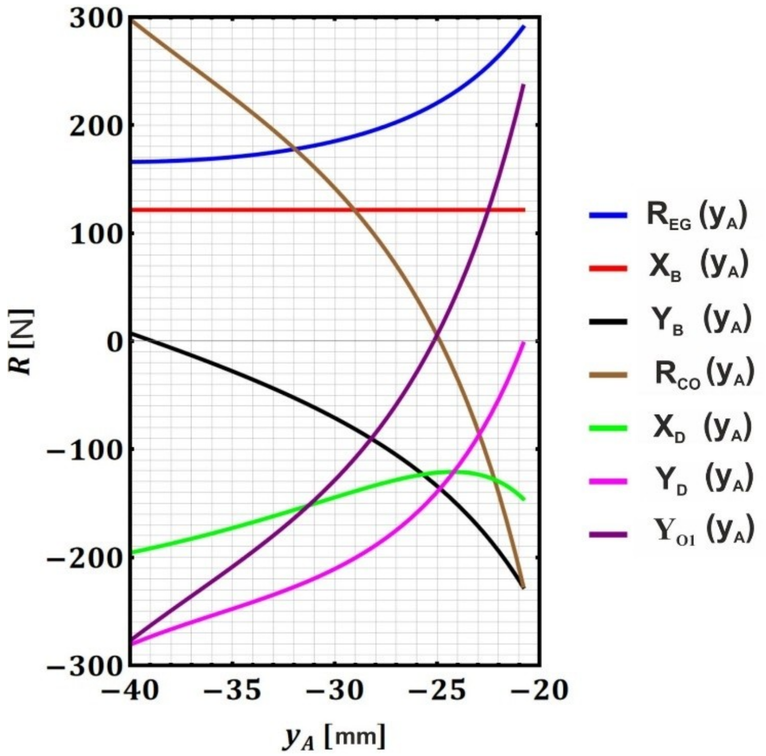

Figure 11: Results of force analysis of the gripper mechanism.

4. Future challenges and prospects

Despite significant progress in the development of pantograph grippers for robotic manipulators, a number of challenges remain that need to be addressed to increase their efficiency, adaptability, and reliability. One key aspect is improving the control of the gripping force without the use of complex sensor systems. The introduction of intelligent control algorithms based on machine learning and adaptive models will allow automatically adjusting the gripping force depending on the shape, material, and mechanical properties of the object [15, 16,17, 18].

Another important area of development is optimizing the gripper design to achieve greater flexibility and versatility. In particular, the use of composite materials and additive manufacturing technologies opens up new opportunities for reducing the structure's weight and improving its mechanical characteristics.

In general, the future development of pantograph grippers will be aimed at combining advanced design solutions with flexible control methods, which will ensure their high performance, reliability, and adaptability to a wide range of tasks in industrial robotics.

5. Conclusion

In this study, robotic gripper design was developed, analyzed, and optimized, providing efficiency, adaptability, and ease of control. It was found that the position of the gripper jaws can be uniquely determined by a single generalized coordinate, which significantly simplifies mathematical modeling and control algorithms.

The results of kinematic and force analysis confirmed the stability and accuracy of the proposed design, which makes it promising for automated production systems and robotic manipulators in industries where reliable and controlled fixation of objects is required. The proposed approach can be used for further improvement of industrial robotic grippers, as well as the integration of intelligent control algorithms for adaptive manipulation of objects of complex shape.

Thus, the analysis and modeling confirmed the effectiveness of the proposed design solution, which provides stability, accuracy, and reliability of gripping in automated production systems.

Declaration on Generative AI

The authors have not employed any Generative AI tools.

References

[1] V. Korendiy, O. Kachur, A. Augousti, and O. Lanets, “Optimizing the structural parameters of the robotic system to ensure the efficiency and reliability of work in the production environment,” *in Proceedings of the 1st International Conference on Smart Automation & Robotics for Future Industry (SMARTINDUSTRY 2024)*, Lviv, Ukraine, Apr. 18-20, 2024, CEUR Workshop Proceedings, vol. 3699, pp. 180–197, 2024. Available: https://ceur-ws.org/Vol-3699/paper13.pdf.

[2] Y. Liu, C. Zhao, Z. Kong, and F. Taghizadeh-Hesary, "Pathways to stable economic policy: The role of industrial robotics and energy transition," *Renewable Energy*, vol. 2025, p. 122751, 2025. doi: 10.1016/j.renene.2025.122751.

[3] V. Kumar, P. J. Coelho, and C. Neves, "A systematic review of developments in gripper technologies for rigid fabric parts," *Heliyon*, vol. 10, no. 22, p. e40387, 2024. doi: 10.1016/j.heliyon.2024.e40387.

[4] G. Monkman, S. Hesse, R. Steinmann, and H. Schunk, Robot Grippers, *Wiley-VCH*, 2007. doi: 10.1002/9783527610280.

[5] M. Xu, Y. Liu, J. Li, F. Xu, X. Huang, and X. Yue, "Review of Flexible Robotic Grippers, with a Focus on Grippers Based on Magnetorheological Materials," *Materials*, vol. 17, no. 19, p. 4858, 2024. doi: 10.3390/ma17194858.

[6] J. Hernandez, M. S. H. Sunny, J. Sanjuan, I. Rulik, M. I. I. Zarif, S. I. Ahamed, H. U. Ahmed, and M. H. Rahman, "Current Designs of Robotic Arm Grippers: A Comprehensive Systematic Review," *Robotics*, vol. 12, no. 1, p. 5, 2023. doi: 10.3390/robotics12010005

[7] H. Jahanshahi and Z. H. Zhu, "Review of machine learning in robotic grasping control in space application," *Acta Astronautica*, vol. 220, pp. 37-61, 2024. doi: 10.1016/j.actaastro.2024.04.012.

[8] Ramish, F. K., Ali, S., & Ali, N. "Design and Development of a Prototype Robotic Gripper,” *arXiv*, May 2021. doi: 10.48550/arXiv.2105.11024.

[9] Universal Robots, Types of Grippers Used in Manufacturing, Universal Robots Blog, 2019. URL: https://www.universal-robots.com/blog/types-of-grippers-used-in-manufacturing/.

[10] Y. Kim, J. Shin, J. Won, W. Lee, and T. Seo, “LBH gripper: Linkage-belt based hybrid adaptive gripper design for dish collecting robots,” *Robotics and Autonomous Systems*, vol. 185, p. 104886, 2025. doi: 10.1016/j.robot.2024.104886.

[11] H. Hua, Z. Liao, and J. Zhao, "Design, Analysis, and Experiment of an Underactuated Robotic Gripper Actuated by Linear Series Elastic Actuator," *Journal of Mechanisms and Robotics*, vol. 15, no. 2, p. 021002, 2023. doi: 10.1115/1.4054609.

[12] Z. Wang, Y. Li, and S. Wang, "Design and analysis of a novel compliant gripper with adjustable stiffness for robotic manipulation," *Robotics and Computer-Integrated Manufacturing*, vol. 79, p. 102401, 2023. doi: 10.1016/j.advengsoft.2022.103366.

[13] Cortinovis, G. Vitrani, M. Maggiali, and R. A. Romeo, "Control Methodologies for Robotic Grippers: A Review," *Actuators*, vol. 12, no. 8, p. 332, 2023. doi: 10.3390/act12080332.

[14] Engineers Edge, Coefficients of Friction, 2025. URL: https://www.engineersedge.com/coeffients_of_friction.htm.

[15] R. Kumar, U. Mehta, P. Chand, "A Low Cost Linear Force Feedback Control System for a Two-fingered Parallel Configuration Gripper," *Procedia Computer Science*, vol. 105, 2017, pp. 264-269. doi: 10.1016/j.procs.2017.01.220.

[16] X. Zhang, Q. Xu, "Design and testing of a novel 2-DOF compound constant-force parallel gripper," *Precision Engineering*, vol. 56, Mar. 2019, pp. 53-61. doi: 10.1016/j.precisioneng.2018.09.004.

[17] P.-L. Chang, I.-T. Chi, N. D. K. Tran, D.-A. Wang, "Design and modeling of a compliant gripper with parallel movement of jaws," *Mechanism and Machine Theory*, vol. 152, Oct. 2020, Art. no. 103942. doi: 10.1016/j.mechmachtheory.2020.103942.

[18] T. Takahashi, K. Yamazaki, S. Saito, H. Kobayashi, "Design and Control of Parallel Gripper with Linear and Curved Trajectory Consisting of Only Revolute Pairs," 2020 IEEE/SICE *International Symposium on System Integration (SII)*, Honolulu, HI, USA, 2020, pp. 557-562. doi: 10.1109/SII46433.2020.9025997.